Detecting Qatar-1b with a Planetary Transit

Uzair Tahamid Siam, Navya Uberoi

January 10, 2022

Abstract

In this project we observe the transit of the exoplanet Qatar-1b using the 24-inch telescope situated in the MEES observatory. With our observational data of the planet we determine its orbital period, $T = 26.938/n$ days with n being the number of orbital cycles apart we observe the planet (from comparing with exoplanet database we find n = 19), and radius, $R = 1.29 \pm 0.05 R_{\text{Jupiter}}$ while considering the effects of limb darkening on the light curve. Additionally we estimate its inclination angle to be around 90° as we could observe its transit. Using its physical properties we also inferred that it is a hot Jupiter that is too close to its host star making its surface extremely hot and uninhabitable. Given its size and orbital radius we also inferred that it could not have formed so close to its star and must have drifted towards it while accreting matter. We finally compared our calculated planetary properties with those found in databases and found our T and R are within 3σ of the database values of $P = 1.4$ days and $R_0 = 1.14 R_{\text{Jupiter}}$

1 Introduction

Questioning the existence of planets beyond our solar system naturally arises as we ponder about the countless stars that we see even with our bare eyes. If our Sun is orbited by a diverse array of planets, is there a chance that every one of those stars we observe has its own array of stars? This has been a question that astronomers have been intruiged by for thousands of years and now with technology we have finally been able to find an answer.While the idea of exoplanets *existing* beyond the solar system has not been an unusual thought, everyone agreed that *detecting* them would be extremely challenging. These planets would not only be incredibly far away and faint, they would also be expected to be outshined by their host star, making it nearly impossible to view them directly through even the most powerful telescopes. Therefore the only way to detect such planets would be through indirect methods.

The earliest of these methods was the search for the reflexive motion of a planet and a star due to the gravitation attraction between each. In 1995, Swiss astronomers Michel Mayor and Didier Queloz detected the first planet, now named 51 Peg-B [1], orbiting a Sun-like star using this reflexive motion. Their detection method involved measuring the Doppler effect of the star's spectrum due to this reflexive motion. From the Doppler shift, they measured its orbital period and its mass. They discovered that 51 Peg-B was unlike any planet we had known about so far, as it was extremely close to the star — even closer than Mercury to the Sun — and was also at least half the mass of Jupiter. This was considered impossible according to the existing planetary formation models. It was later found that the model was, in fact, not wrong. The planet, much like Jupiter, is thought to have formed much farther away from its host star and may have slowly drifted towards the star in the absence of other strong gravitational sources close by. Stars like these are now classified as Hot Jupiters.

However, there was still much skepticism in these discoveries as these could also be the result of other stellar phenomena like star pulsations and star spots. This skepticism was put to rest in 1999 when HD 209458b was discovered [2]. This planet was orbiting edge-on to the Earth and as a result we were able

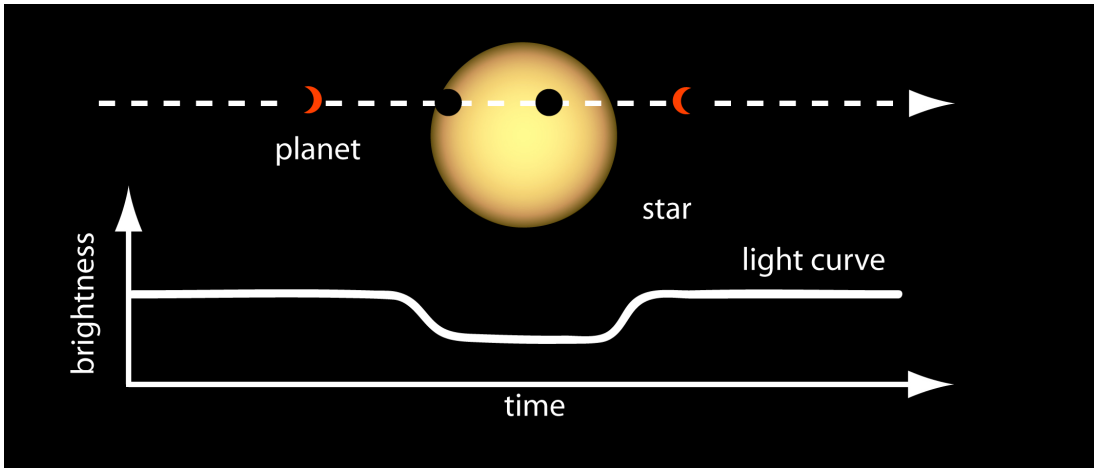

Figure 1: Schematic of a transit curve

to see the planet directly in front of its host star. Using this transit of the planet in front of its star, we could not only show that exoplanets do exist but also learn about several physical properties of the planet by studying the spectrum of the star during the transiting period. Now, with the planet's mass from the Doppler shift and the planet's radius from the transit method, we could calculate the densities which would tell us whether the star is gaseous or rocky which would allow us to classify exoplanets more of which were bound to be found. Finally, in 2009 NASA launched Kepler which found 1000 confirmed exoplanets by early 2015.

In our project we aim to study the properties of one of these known exoplanet using the transit method and compare our findings with that in exoplanet databases.

2 Instruments and Targets

2.1 The Telescope

The telescope used in this project [5] is located in the University of Rochester's C.E.K. Mees Observatory, 40 miles south of Rochester in the Bristol Hills (77°24'31.56" W, 42°42'01.0" N) at an elevation of 701 m (2260 ft). The 24-inch Cassegrain telescope by DFM engineering installed in 1965 has f/13.5, plate scale 25.1 arcsec/mm in the Cassegrain focal plane. The large CCD covers 0.224 arcsec/pixel in 1x1 binning, 15.4 arcmin on a side, 21.7 arcmin diagonal. The autoguider CCD: 0.259 arcsec/pixel, 2.8x2.1 arcmin. It has an unvignetted field of view 24 arcmin in diameter and collecting area: 2700 cm^2 = 0.27 m^2.

Facility focal-plane instruments include:

- an SBIG STX-16803 CCD camera (4096x4096 pixels, 15.4 arcmin square field of view), with an internal autoguider and a complement of broadband - L, R, G, B which have peak $\tau \geq 0.95$ - and spectral-line filters - [O_{III}], H_α, [S_{II}] all of which have peak $\tau = 0.85 - 0.9$ and FWHM, $\Delta\lambda = 8.5, 7.0, 8.0$ nm respectively where τ is a transmission coefficient ranging between 0-1.
- a Shelyak LHiRes III grating spectrograph (resolving power up to 18000) with a slit-viewing video camera and an SBIG ST-7 focal-plane camera.

2.2 Target: Qatar-1b

In our project we observe the transit of the exoplanet, Qatar-1b. Qatar-1b is an exoplanet orbiting a K-type host star, Qatar-1, which has V magnitude = 12.42, radius R = $0.803 \pm 0.01 R_{\text{Sun}}$, mass M = $0.838 \pm 0.042 M_{\text{Sun}}$, and temperature T = 5013 ± 91K [3]. We wish to observe the a dip in the flux of this star, as shown schematically in Fig. 1, and prove that this dip could only be a result of an exoplanet transit. Furthermore, we wish to determine some of the exoplanet's physical properties, such as its classification i.e. if it is a hot Jupiter or a rocky planet, and if it might be habitable.

3 Data Collection

Since, there were no clear nights towards the end of April 2021, we did not have a chance to observe with the telescope. Instead, we used data collected by Prof. Dan Watson on October 13 and November 9, 2020. As a result, we will be writing about what Prof. Watson has logged into the Mees observation log book and address some of the problems he encountered.

Since we are only interested in the variation of the total flux from the host star, we only take data in the Luminance filter with 2x2 binning. The host star, Qatar-1, was observed with 300s exposure for October 13 and 240s for November 9. Qatar-1b was likely chosen because it is bright enough to not require longer than 300s exposures in L to ensure that enough images could be taken over the span of its transit to analyze it.

The first set of observations was made remotely from the River Campus at the University of Rochester on the night of October 13, 2020. The temperature at C.E.K. Mees Observatory was recorded to be 60°F with winds around 10 mph. The sky was reportedly clear but with heavy smoke and clouds started coming in at around 8:20 PM EDT.

Typically, a night of observation begins with taking flat field images in all filters to map the dust pattern on the camera, but due to technical issues that cannot be done remotely. So, the telescope was started up, zenith was initialized, equatorial track rate was set to 15.02 arcsec/sec. The telescope was then connected to the software TheSky, which is used to slew the telescope to a desired target in the sky. The telescope pointing was initialized by selecting a bright star near zenith and taking a short exposure image in the Luminance filter (L-band) with 2x2 binning. The star was identified in the frame, and the telescope offset was adjusted such that it the target is in the center of the frame.

Next, the telescope was focused using a star that is neither too bright or too dim. The telescope's focus position was set to its maximum possible value 4000, with the intention of bringing it down incrementally till the appropriate focus position is found. We assume Prof. Watson took 30s exposures of the star in the L band with 2x2 binning, decreasing the focal length in increments of 50 after each exposure was completed. Each image of the star has a maximum pixel value and half-flux diameter associated with it; the focus value corresponding to the image with the greatest maximum pixel value and least half-flux diameter is selected as the telescope's focus for the night, which turned out to be 3320. The half-flux maximum of the star was found to be 5.58 arcsec; multiplying this number by 0.448 gives the seeing for the night, which was 2.5 arcsec.

Finally, the telescope was slewed to the target, Qatar-1. Since more than 4 minutes of exposure time was required to get a good signal-to-noise ratio, Autoguiding would have to be set up. A guide star would have to be identified close to the field around the target, located in the telescope's Autoguider periphery. The camera would be set to take 30s-60s exposures of this star in the L band with 1x1 binning until aborted, so that it can continue to point towards the same object in the sky and keep the target in the frame. Then, a series of images for our target was set up — 300s exposures were taken in the Luminance filter with 2x2 binning, ensuring that the total observing period spans the entirety of the exoplanet transit.

The second set of observations was made remotely on the night of November 9, 2020. This time the temperature was 63°F but the winds were much calmer at 5 mph. Similar steps were carried out to start the telescope and initialize it, and the focus was found to be 3350 while the seeing was 2.5 arcsec. The tracking rate was also set to 15.02 arcsec/sec. However, during this observation the exposure time was reduced to

240 sec, as the star was looking overexposed with 300s, and according to the log book the transparency and seeing appeared to be better than 13th October.

4 Data Processing

Before we can analyze our targets, we need to perform a series of steps that reduce the signal-to-noise of our images and correct for any transients. These steps comprise the data reduction process. The very first step is to calibrate our images using Master dark and bias fields taken in January 2021, which subtract the effects of dark and bias current from our frames. To do so, we use the software CCDStack, which allows us to open a series of images in a single stack, and perform actions on them at the same time. For each target, we open all the L images together in the same stack, and apply the 2x2 binning Master bias and dark subtraction to all images in this stack. Additionally, we removed all hot and cold pixels in the images. Finally, after calibration we identified our star in the images as shown in Fig. 2.

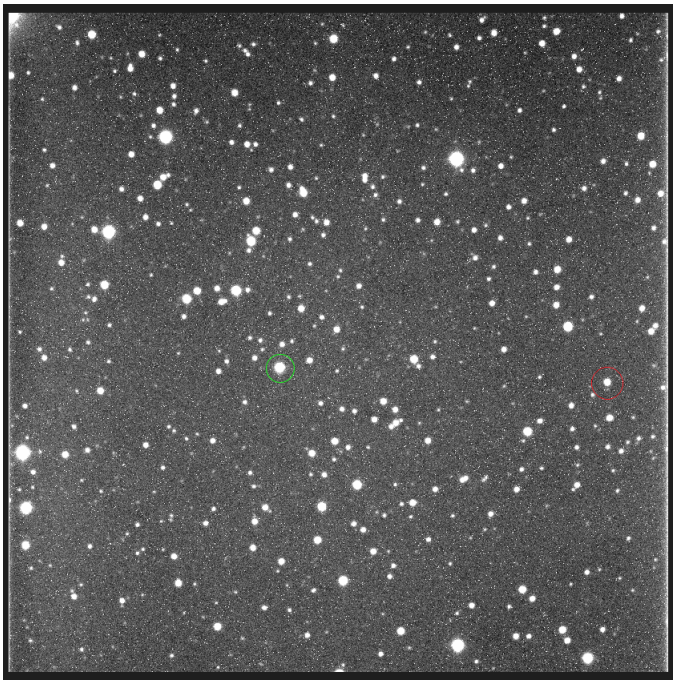

Figure 2: The stellar field around Qatar-1, as observed through the telescope. The target star is circled in green and the reference star is circled in red.

For the next step, the atmospheric extinction was to be corrected for each image. As an object moves further away from zenith, its light passes through more layers of the atmosphere, resulting reduced signal. However, in our analysis, we are only interested in the "dip" of the flux of target as a function of time; we do not need the exact signal. Therefore, we can simply divide the flux of our target by the flux of a bright, non-pulsating star in our frame to get a normalized flux. Since both the target and the reference star are at almost the same altitude, the atmosphere affects the signal from both stars equally. Therefore, taking the ratio of the fluxes cancels out the effects of atmospheric extinction.

5 Data Analysis

With our data processed we now move on to the analysis process. To find the fluxes of our target star and reference star, we use ATV, a part of the IDL image-processing language. ATV is a user-friendly point-and-click aperture photometry tool which can produce high quality output images. We open each image one-by-one in ATV and inverted the Y axis to better identify our two stars in the frame. The tools used are represented in Fig. 3 below.

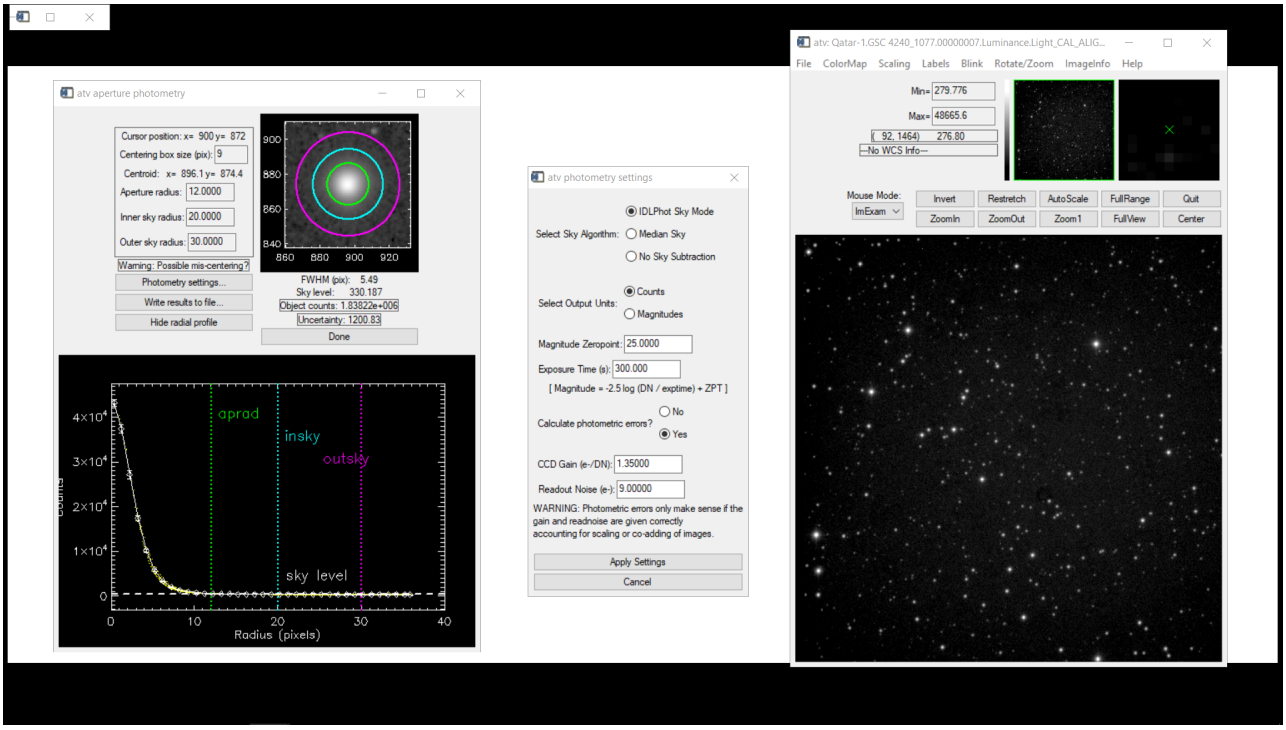

Figure 3: Visual representation of ATV flux determination process and tools

In the "ImExam" mode, we click on our reference star, which opens up a Photometry window centered on it. We adjust the aperture radius such that it contains the entire signal from the star, and adjust the inner and outer sky radii to define the background annulus. ATV also calculates the photometric error in the signal using the CCD gain (1.35 e^{-1}/DN) and the readout noise (9 e^{-1}), and the FWHM which can be multiplied by 0.448 to find the seeing in 2x2 binning. We note the signal from the star, which is in units of Data Numbers (DN). We then click on our target, and ensure that we use the same aperture radius to get consistent readings while still capturing the entire flux from the star. At every step of the process, we make sure that the signal-to-noise ratio was high. Additionally, we note the time the images were taken at in decimal days, or the number of days passed since the very first image was captured (9:38 PM EST on 10/13/2020). We repeat this process for all images in the stack.

To find the normalized flux of our target, we divided the flux of our target by the flux of our reference star. The uncertainty in this normalized flux was computed for each frame using the standard error propagation formula:

$$\sigma_{\text{norm}} = \sqrt{\left(\frac{1}{f_{\text{ref}}}\sigma_{\text{star}}\right)^2 + \left(\frac{f_{\text{star}}}{f_{\text{ref}}^2}\sigma_{\text{ref}}\right)^2} \tag{1}$$

where f_{star}, σ_{star} and f_{ref}, σ_{ref} refer to the flux and associated uncertainty of the target star and reference star in each frame respectively.

Additionally, we further normalized these fluxes by setting the value of the baseline flux to one. This ensures uniform comparison between the data from the two nights. To do so, we select the points that we believed comprised the baseline flux and not the transit for each night separately. Since this process is arbitrary, we reported the mean of these flux values as our normalizing factor, and the standard deviation as the associated uncertainty. We then divided the flux of all our data points by this factor. The resulting uncertainty in each data point was found by propagating the standard deviation of the normalizing factor with the uncertainties computed in the earlier step.

For each night, we plot the normalized flux of our target star as a function of this decimal days from the first image. The plots are shown in Fig. 4.

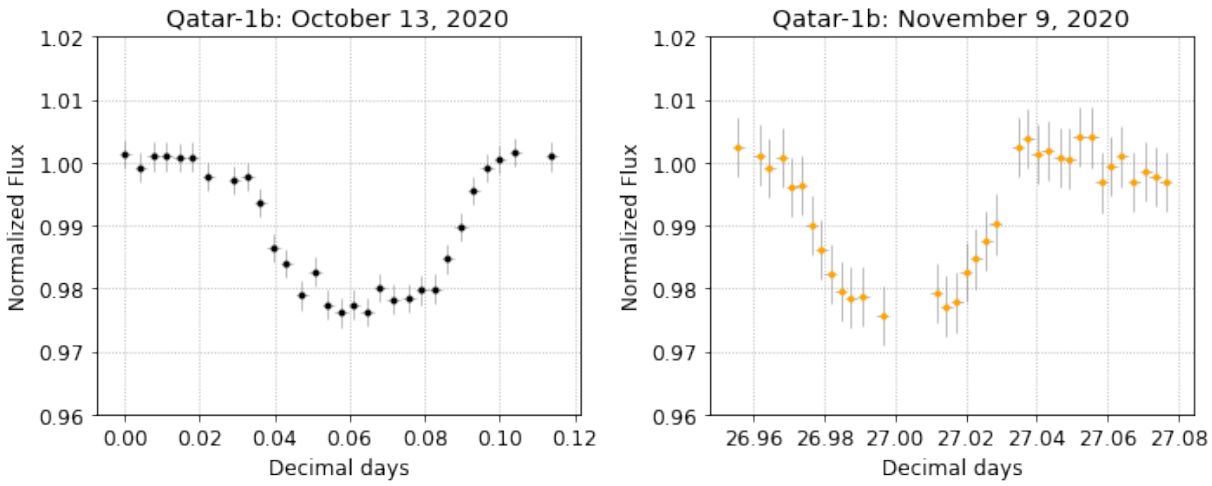

(a) (b)

Figure 4: Flux vs time light curves for the two nights of observations.

Since our data spans two nights, we phase fold the curves to get a single curve as shown in Fig. 6. Phase folding is the process wherein we line up two curves by shifting the x-axis by a value that is the multiple of the period of variability. This allows us to compute the period to a reasonable extent, as well as obtain perform analyses on a single curve with more data as opposed to separate curves. We carried out this process by simply shifting back the x-axis of the data from November 9 until it aligned with the data from October 13. We discovered that this shift was 26.938 days; this implies that the period of variability of our data is an integer dividend of this value. We further those to center our phase-folded curve such that the middle of the transit corresponds to zero.

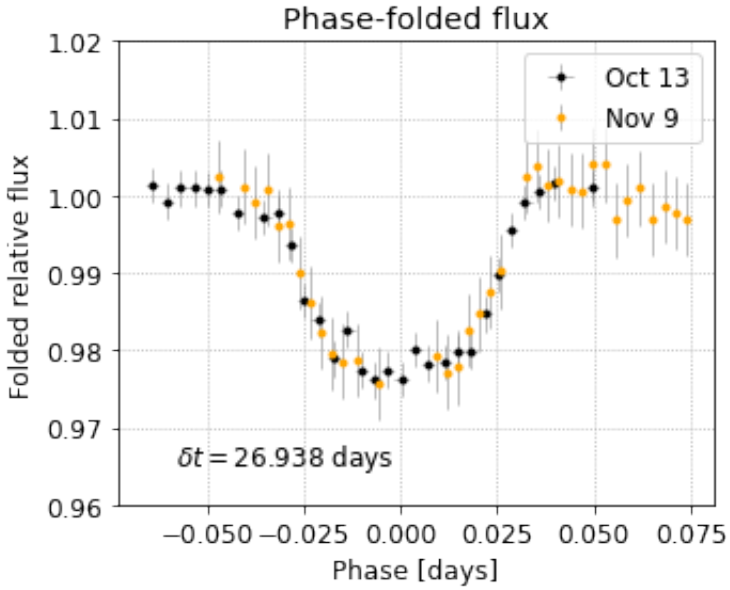

Figure 5: Phase-folded light curve with a phase shift of $\delta t = 26.938$d. The shaded regions represent the errors and the solid line gives the depth and the times

We had to shift some of the data points along the flux axis on the November 9 data because the fluxes were translated down by a constant value. This was likely a result of some of the problems faced during data collection as mentioned before, such as thin passing clouds. Given that all points in those frames were off by the same value from the October 13 data, we believe that it was a normalization error that we could fix without having to worry about unjustifiable data manipulation.

Our phase-folded curve closely resembles the schematic diagram from Fig. 1. Assuming that it is indeed a planetary transit (the possibility of which is discussed in later sections), we wish to determine the start and end times of the transit. The beginning of the transit, where the flux of the star is decreasing, is called the ingress, while the second half where the fluc is increasing is called the egress. We let t_a and t_b be the start and end time of the ingress, and t_c and t_d to be the start and end time of the egress. It is not trivial to simply look at the curve and pick out the values of these times. Instead, we devise a systematic method that not only gives us a reasonable value of these times, but also some bounds on its uncertainty.

To find t_a, we first identify a few points near the region where the flux just started decreasing. We determine the mean of the x-values of those points and calculate the standard deviation. Therefore, the mean x-value can be reported as the value of t_a and its associated uncertainty is then the standard deviation. Similarly, to find t_b, we identify points where the flux just started to stabilize, and the mean and standard deviation of the x-values of those points was reported as t_b and its uncertainty. The same process was carried for t_c and t_d, and the values we obtain are reported in Table 1.

	phase/days	error/days
t_a	-0.033	0.004
t_b	-0.016	0.003
t_c	0.018	0.004
t_d	0.034	0.008

Table 1: Tabulated ingress/egress phase time shifts and their respective errors. The negative values are a consequence of centering the light curve at phase = 0.

Another parameter we would like to measure is the dip in the flux. We assume that all the points contained between t_b and t_c make up the dip; therefore, the average phase of those points can be considered our minimum flux, and the standard deviation is reported as the uncertainty in this flux. The total uncertainty in this value is computed by adding this standard deviation and the individual uncertainties in each points in quadrature. We find that the minimum flux is measured to be 0.977±0.002, which means that the depth of the transit is roughly 2.3%.

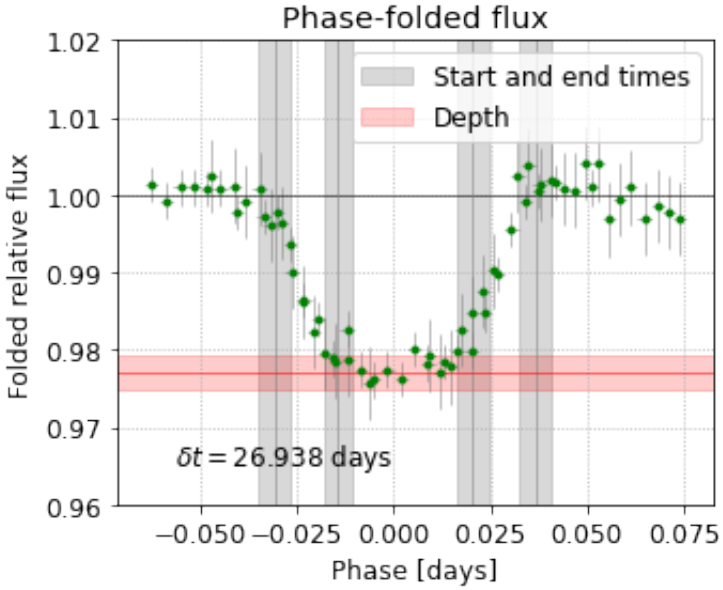

Figure 6: Phase-folded light curve with a phase shift of $\delta t = 26.938$d

One would note, as in Fig. 6, that the uncertainty ranges are not small by any means. One also notes that the curve we obtain is not a trapezoid-like curve with a sharp ingress and egress. What we observe is a relatively smoother transition into the transit, and a slightly curved dip in the minimum flux. This occurs due to a phenomenon known as stellar limb darkening. The flux of a star, when viewed from Earth, is not constant as a function of the radius of the star. In fact, the edge of the star appears cooler or dimmer than the center, with the flux increasing as we move towards the center. While the precise mechanism of stellar limb darkening is not relevant to this analysis, what we must consider is that as the exoplanet passes in front of the star, it travels through a region of variable flux as opposed to constant flux. This results in the smoother curves and dips that we see in the phase-folded graph. Additionally, this also explains why our error margin are large — since the flux is not strictly constant or similar at any point, we cannot pin down a single value for the start and end time of the ingress or egress.

6 Transit and The Planet

6.1 The transit

Before moving on to discuss the properties of the planet itself, we address the skepticism of whether it is truly a planetary transit or some other stellar phenomenon. We consider three of the other most common phenomena that include the concept of variable fluxes in time, and discuss why our light curve can only be that of a exoplanet's transit.

- **Stellar variability:** Pulsating variable stars are intrinsic variables as their variation in brightness is

due to a physical change within the star. In the case of pulsating variables, this is due to the periodic expansion and contraction of the surface layers of the stars. This means the star actually increases and decreases in size periodically. The different types of pulsating variables are distinguished by the shapes of their light curves, all of which have a saw-tooth profile, which is distinctly absent from our data. Furthermore, pulsating stars do not have a long duration at which they emit a "baseline" flux; our transit, on the other hand, starts and finishes within the short duration of observation (less than two hours). This leads us to believe that the flux variation we observe could not be the result of variations in the star's intrinsic brightness.

- **Starspot:** When a starspot is observed, the light curve's periodicity depends completely on the rotational period of the star itself. The rotational period of a star is much longer than the transit period of a planet. The star that Qatar-1b orbits is a K type star which has rotational period ranging from 0.2 - 70 days, while our transits only span over 1.61 hours. Additionally, it is unlikely for a starspot to decrease the brightness of the star by 2.3%. This indicates that it is highly unlikely that the variability we observe is due to a star spot on Qatar-1.

- **Eclipse in a binary star system:** The light curves of eclipsing binary star systems is expected to have several dips in the flux in rapid succession, with some of the dips in flux being deeper than the others but neither as deep as those seen during planetary transits given both stars still emit their own light, unlike a planet. Again, we can agree that our light curve cannot represent an eclipsing binary system given we only have one dip throughout the transit.

6.2 Properties of the Exoplanet

Now that we have convinced ourselves that we are indeed looking at a planetary transit, we use our light curve to infer some of the physical properties of the planet. From the phase-folded plot above, we have found the period to be 26.938 days. However, that period must be divided by some positive integer n to take into account the possibility that we observed the orbital period after a certain number of cycles. Therefore, we conclude that the period is given by:

$$T = \frac{26.938}{n}\text{days} \tag{2}$$

Next, to find the radius of the planet, we first need to know the radius of the star. However, using transits it is not possible to learn about the host star's radius and we usually have to rely on Doppler velocity to compute that. Therefore, we find the typical radius of K-type , which we found to be $0.803 \pm 0.01 R_{\odot}$.

There are two ways we can determine the radius of planet; one way uses the depth of the transit, while the other uses the ingress and egress times. The first method yields us:

$$\left(\frac{R_{\text{planet}}}{R_{\text{star}}}\right)^2 = d \Rightarrow R_{\text{planet}} = \sqrt{d} \cdot R_{\text{star}} \tag{3}$$

where d is the depth of the transit. The other method is given by:

$$R_{\text{planet}} = \left(\frac{t_b - t_a}{t_c - t_a}\right) R_{\text{star}} \tag{4}$$

Equation 6.2 has an in-built assumption that the inclination angle is 90°. This is usually true for exoplanets that are observed using the transiting method; we can therefore assume that Qatar-1b, too, has a an orbital inclination close to 90°. We find our planet radii to be $1.13 \pm 0.05 R_{\text{J}}$ using Eq. 6.2 and $1.99 \pm 0.122 R_{\text{J}}$ using Eq. 6.2 (where R_{J} is the mass of Jupiter).

There is some discrepancy between these numbers. Note that the answer computed using Eq. 6.2 uses only one computed parameter, while Eq. 6.2 uses three, all of which are computed using our own analysis

methods and have built-in systematic uncertainties. Furthermore, Eq. 6.2 also depends on the angle of inclination [4], which can lead to small but non-negligible inaccuracies. Therefore, we believe that the radius of the exoplanet computed using Eq. 6.2 should be a better estimate.

It is also important to consider the effects of stellar limb darkening in this analysis, which is one of the key reasons for larger uncertainties in our estimation of the radius of the planet. A lot of literature can be found where the limb darkening coefficient is characterized in terms of the temperature, metallicity and other properties of the star. However, as mentioned earlier, we have decided to roughly approximate the consequence of limb darkening by taking the standard deviation around the average flux value of points that lie between $t_b$andt_c as the uncertainties in these values.

As mentioned above, the inclination angle of the orbit of Qatar-1b is likely to be around 90° given we can use planetary transit method to observe it. If the inclination angle was too far off from 90° it would be impossible to observe it using this method. This is because the inclination angle is defined as the angle between our line of sight and the orbital axis of the star-exoplanet pair and if the planet is not edge on, we will not be able to see its transit.

We next classify the type of the planet using its size and its orbit. From the orbital period we can infer how close or far the planet is to its star using Kepler's third law ($T^2 \propto a^3$). Since our period T is a function of n, if n is larger it suggests that our T is small and so is our a and vice versa. To get our value of n we make a quick comparison with the orbital period found in databases (1.4 days) and find that n 19, i.e. we observed the planet 19 orbital cycles apart. Given that its orbital period is so short and it is about the same size as Jupiter, it must be a hot Jupiter. Additionally, we can also see that it exists very close to its host star, so the temperature on the gaseous surface of Qatar-1b will most certainly be extremely high for any life to occur, making it uninhabitable. Planets that are the size of Jupiter cannot form this close to its star according to our current planetary formation model because there is not enough material to accrete into such a massive body so close to the star. Much like Jupiter, it must have formed farther away from the star and slowly drifted towards the star while accreting material until it had nothing more to accrete.

We conclude the project by comparing the values we found for the properties of the planet using our observations to those found in exoplanet databases. As mentioned previously our calculated period, $T = 26.938/n$ days represents the same period as that found in databases of $P = 1.4$ days because they are approximately off by an integer multiple of n = 19. So, our period value agrees with the true value within 3σ. The radius, $R = 1.13 \pm 0.05 R_{\text{Jupiter}}$ also is within 1σ of the true radius of Qatar-1b, $R_0 = 1.14 R_{\text{Jupiter}}$.

7 Conclusion

Our dry lab analysis of the transit of Qatar-1b using Prof. Dan Watson's data from two nights allowed us to study important properties of the planet and discuss the habitability conditions of the planet Qatar-1b orbiting the K-type star Qatar-1. We believe that we managed to analyze data that was of high quality, despite issues with clouds and haze on the day of observations. In all our readings, we were able to reach the desired levels of signal-to-noise ratio and ensure we reached the expected photometric accuracy.

Using the phase-folded light curve generated by the fluxes from the images taken and taking into consideration the effects of limb darkening, we find the ingress and egress times and also the depth of the light curve. We ruled out other possible variability effects, such as starspots and pulsating star. We then find the planetary and orbital properties such as a period of $T = 26.938/n$ days (where we find n to be 19 by comparing our data with known period), the radius of the planet, $R = 1.29 \pm 0.05 R_{\text{Jupiter}}$, and an estimate of its inclination angle, $i \approx 90°$. From these calculations we also infer the type of the planet as a hot Jupiter, find its relative formation position to be far as a Jupiter size planet cannot form very close to the star, and also make comments about how the surface is too hot to be habitable. Finally, to check whether our analysis of the properties of Qatar-1b were comparable to those found in existing databases, we compared results and found our T and R are within 1σ of the database values of $P = 1.4$ days and $R_0 = 1.14 R_{\text{Jupiter}}$.

References

[1] Mayor et. al. **?**A Jupiter-mass companion to a solar-type star**?** In: *Nature* 378 (1995), pp. 355–359. DOI: https://doi.org/10.1038/378355a0.

[2] David Charbonneau et al. **?**Detection of Planetary Transits Across a Sun-like Star**?** In: 529.1 (Jan. 2000), pp. L45–L48. DOI: 10.1086/312457. arXiv: astro-ph/9911436 [astro-ph].

[3] Karen A. Collins, John F. Kielkopf, and Keivan G. Stassun. **?**Transit timing variation measurements of WASP-12b and Qatar-1b: No evidence of additional planets**?** In: *The Astronomical Journal* 153.2 (Jan. 2017), p. 78. ISSN: 1538-3881. DOI: 10.3847/1538-3881/153/2/78. URL: http://dx.doi.org/10.3847/1538-3881/153/2/78.

[4] Brett M. Morris et al. **?**Robust Transiting Exoplanet Radii in the Presence of Starspots from Ingress and Egress Durations**?** In: *The Astronomical Journal* 156.3 (Aug. 2018), p. 91. DOI: 10.3847/1538-3881/aad3b7. URL: https://doi.org/10.3847/1538-3881/aad3b7.

[5] University of Rochester. *C.E.K. Mees Observatory*. URL: https://www.sas.rochester.edu/pas/about/observatory.html.